Noncovalent Binding of Some New Lipophilic Gadolinium DTPA Complexes to Human Serum Albumin. A Structure–Affinity Relationship

by **Sophie Laurent**, **Luce Vander Elst**, **Virginie Henrotte**, and **Robert N. Muller***

Department of General, Organic and Biomedical Chemistry, Laboratory of NMR and Molecular Imaging, University of Mons, 19 Avenue Maistriau, B-7000 Mons
(phone: +32-65-373520; fax: +32-65-372533; e-mail: robert.muller@umons.ac.be)

Four Gadolinium·DTPA complexes bearing long lipophilic alkyl chains were synthesized: two bis[amide] and two 4-substituted derivatives. In two of them (one bis[amide] and one 4-substituted), the alkyl chain ends with a carboxylate function. Their relaxometric properties in H_2O show the self aggregation of Gd·DTPA-BdodecylAmide, the better stability of the 4-substituted derivatives *vs.* Zn transmetallation, and the very good stability of Gd·(4-(carboxyundecylisothiourea-Bz)DTPA). Amongst the four compounds, only Gd·(4-(carboxyundecylisothiourea-Bz)DTPA) shows a strong interaction with human serum albumin (HSA) as demonstrated by proton relaxometry and ESI mass spectrometry. These data highlight the importance of the negative charge on the alkyl chain in the context of the interaction of Gd·(4-substituted DTPA) derivatives with HSA.

Introduction. – Magnetic resonance imaging (MRI) is a powerful and non-invasive technique routinely used in medical diagnosis. However, some examinations require the use of contrast media. Most of the clinically used MR contrast agents are compounds containing a paramagnetic ion capable of enhancing the relaxation rates of the H_2O H-atoms of tissues where they accumulate. In this way, they enable the characterization of lesions and abnormalities in tissues and blood vessels. Gadolinium chelates are the most widely used T_1-agents. For clinical use, the recommended dose is 0.1 mmol/kg. Because of their low molecular masses, they diffuse in the interstitial space – and, therefore, their biodistribution is nonspecific – and are rapidly excreted by the kidneys. To overcome the problem of rapid clearance, complexes of Gd with reversible binding to blood proteins have been developed. The theory behind these agents is that the reversible binding allows an extended blood half-time and reduces the fraction of free chelate available for glomerular filtration in the kidneys. In addition, the binding to a macromolecule results in an increase of the rotational correlation time of the Gd chelate leading to an enhancement of its efficiency. For example, MS-325 (*Vasovist*®), developed by *Lauffer et al.* [1], consists of a diphenylcyclohexyl group attached to Gd·DTPA (diethylenetriamine-*N*,*N*,*N*′,*N*′,*N*″-pentaacetic acid) by a phosphodiester linkage. The presence of the lipophilic group allows the noncovalent binding to human serum albumin (HSA). The reversible binding leads to a high relaxivity (the relaxivity is defined as the relaxation rate enhancement produced by one mmole per l of the paramagnetic compound) [2][3] and, as a result, a low dose of 0.03 mmol/kg produces excellent blood–tissue contrast enhancement. In humans, MR angiography with MS-325 has shown to provide a safe and effective evaluation in phase

III studies [4]. Competition studies with fluorescent probes suggested that MS-325 binds primarily to site II of HSA in accordance with the *Sudlow* nomenclature [5]. In fact, the three-domain structure of the protein provides a variety of binding sites. The main binding sites were denoted site I and site II: site I corresponds to the hydrophobic pocket in subdomain IIA, and site II to the pocket within subdomain IIIA. Bulky heterocyclic anions with the charge located at a fairly central position in the molecule were usually identified as binding to site I. Neutral aromatic compounds or anionic aromatic structures with the charge located more peripherally (like MS-325) were usually identified to bind to site II.

To study the importance of the hydrophobic character and of the charge of contrast agents with regard to their affinity for HSA, four substituted paramagnetic DTPA complexes with an hydrophobic alkyl chain longer than ten C-atoms introduced through bis[amide] functions or at C(4) were synthesized: Gd·DTPA-BdodecylAmide (Gd·**1**), Gd·DTPA-BcarboxylundecylAmide (Gd·**2**), Gd·(4-(dodecylisothiourea-Bz)DTPA) (Gd·**3**), and Gd·[4-(carboxylundecylisothiourea-Bz)DTPA] (Gd·**4**). The complexes were characterized *in vitro* in aqueous solution and in the presence of HSA. Their stability was studied by transmetallation with Zn ions in phosphate buffer, and their affinities for HSA were evaluated by two techniques, proton relaxation rate measurements and ESI mass spectrometry.

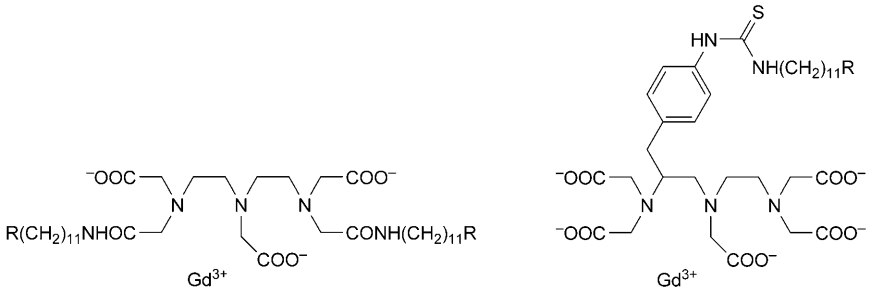

Gd·**1** R = Me
Gd·**2** R = COO⁻

Gd·**3** R = Me
Gd·**4** R = COO⁻

Results and Discussion. – *Synthesis.* DTPA-BdodecylAmide (**1**) and DTPA-BcarboxyundecylAmide (**2**)[1]) were obtained by reaction of the DTPA-bisanhydride with dodecanamine and 12-aminododecanoic acid, respectively, as described by *Kimpe et al.* [6] (*Scheme 1*). The ligands 4-(dodecylisothiourea-Bz)DTPA (**3**) and 4-(carboxyundecylisothiourea-Bz)DTPA (**4**)[1]) were synthesized as described in [7] by reaction of 1-(4-isothiocyanatobenzyl)diethylenetriaminepentaacetic acid and the corresponding amine (*Scheme 2*). All these ligands were then complexed with $GdCl_3$.

*Proton Relaxation in H_2O Bisamide Derivatives Gd·***1** *and Gd·***2**. Because of the low solubility of Gd·**1** in H_2O, the proton longitudinal relaxation rates were recorded in a solution of EtOH/H_2O 5:95. *Fig. 1* shows the paramagnetic relaxation rates R_1^p (R_1^p is defined as the observed relaxation rate minus the proton relaxation rate of the solvent)

[1]) For systematic names of the ligands **1**–**4**, see *Exper. Part.*

Scheme 1. *Synthesis of DTPA-BdodecylAmide* (**1**) *and DTPA-BcarboxyundecylAmide* (**2**)

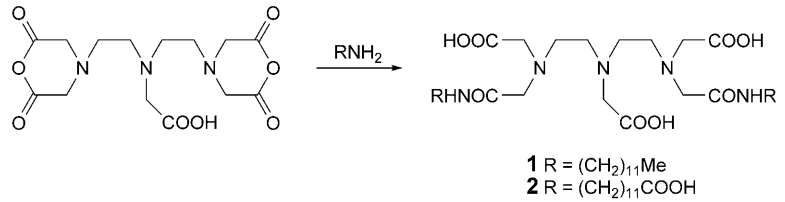

Scheme 2. *Synthesis of 4-(Dodecylisothiourea-Bz)DTPA* (**3**) *and 4-(Carboxyundecylisothiourea-Bz)DTPA* (**4**)

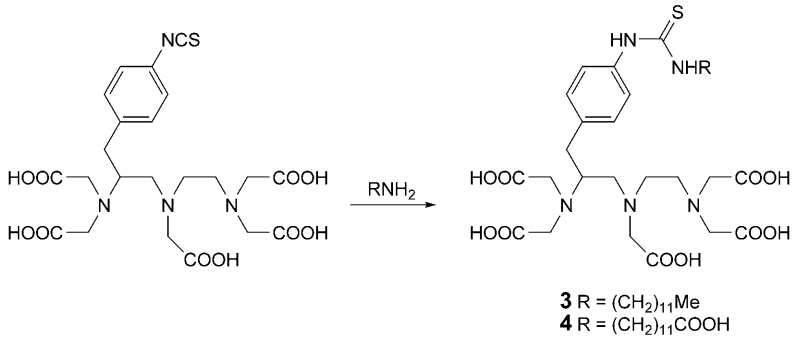

for all complexes recorded over a field range extending from 0.24 mT to 1.4 T. The nuclear magnetic relaxation dispersion (NMRD) profile of Gd·**1** (*Fig. 1,a*) exhibits a marked increase of R_1^p, as compared to the parent complex Gd·DTPA, and a maximum around 20 to 60 MHz. This hump is characteristic of a decreased rotational mobility of the paramagnetic Gd complex and can be explained by the formation of spontaneous micelles in the solution. The theoretical fitting of these data cannot be accurately performed, since the size of the micelles is not controlled. Nevertheless, one can estimate from the high-field data that the mean τ_R is in the ns range.

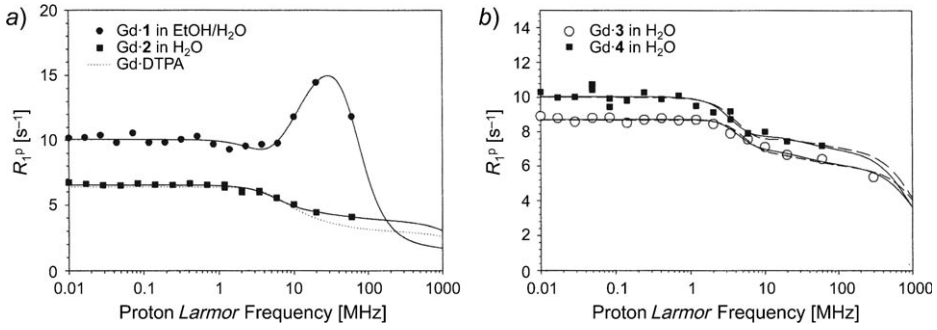

Fig. 1. *NMRD Profiles of the four complexes at a concentration of 1 mM in H_2O at 310 K.* The plain and the dashed lines were obtained by fitting the data with *r* values equal to 0.31 and 0.30 nm, respectively.

As expected, the less hydrophobic Gd·**2** is more soluble in H_2O, and its NMRD profile (*Fig. 1,a*) obtained at a concentration of 1 mM has a the classical shape of a low-molecular-weight Gd complex with a relaxivity at 20 MHz of 4.4 s^{-1} mM^{-1}. The theoretical fitting of the data according to the model of inner- and outersphere paramagnetic contributions [8–10] gives a τ_R value of 94 ps (*Table*) in good agreement with the expected value for a non-aggregated structure. The presence of carboxylate groups on the alkyl chain thus efficiently prevents the formation of micelles in solution and increases the solubility.

Table. *Parameters Obtained by the Theoretical Fitting of the Relaxometric Data.* The following parameters were fixed: $D = 3 \cdot 10^{-9}$ m^2 s^{-1}, $d = 0.36$ nm, $q = 1$.

r [nm]	Gd·**2**[a])	Gd·**3**[b])		Gd·**4**[b])	
	0.31	0.31	0.3	0.31	0.3
τ_R [ps]	94±4	149±3	121±2	179±4	150±3
τ_{SO} [ps]	84±2	85±1	73±1	105±2	87±1
τ_V [ps]	19±2	39±2	32±2	40±2	31±2

[a]) $\tau_M = 1500$ ns. [b]) $\tau_M = 100$ ns.

*4-Substituted Benzyl Derivatives Gd · **3** and Gd · **4***. The R_1^p values of Gd·**3** and Gd·**4** in H_2O at a concentration of 1 mM are greater than that of the parent complex over the whole frequency range (*Fig. 1,b*) with relaxivities at 20 MHz of 6.7 and 7.2 s^{-1} mM^{-1}, respectively. The absence of humps around 20 MHz excludes the formation of large aggregates. The fitted parameters (*Table*) of both complexes were obtained by setting the τ_M value at 100 ns, a value close to those obtained for other Gd·(4-substituted DTPA) derivatives [2][11–14]. Two values of r (0.3 and 0.31 nm) were used. Although the quality of the fittings is quite similar, the τ_R values seem more reasonable for an $r =$ 0.3 nm. The larger τ_R value of Gd·**4** can be related to the presence of the hydrated carboxylate group.

Stability. In phosphate buffer, no significant change of the relaxivity was observed, indicating that the complexes are stable in this medium. The possible transmetallation process by Zn ions was then assessed by measuring the evolution of the R_1^p value of a phosphate solution buffered at pH 7.0 containing equimolar amounts of Gd complex and Zn^{II} ions (2.5 mM). The evolution of R_1^p allows estimation of the extent of the transmetallation process. After *ca.* 500 min, *ca.* 98% of Gd·**1** is dissociated, whereas the dissociation can be evaluated to be 26% for Gd·**2**, and much lower for complexes Gd·**3** and Gd·**4** (18 and 2%, resp.; *Fig. 2*). As already reported [15][16], bisamide derivatives of Gd·DTPA are less stable than 4-substituted derivatives. However, the presence of the carboxylate groups on the alkyl chains greatly enhanced the stability of Gd·**2** probably because of their interaction with the Zn ions. Similarly, the better stability of Gd·**4** as compared to Gd·**3** can be related to the presence of the carboxylate group of the alkyl substituent which can interact with the Zn cation. As compared to the parent compound Gd·DTPA, Gd·**2**, Gd·**3**, and Gd·**4** are more stable regarding the Zn transmetallation process. Moreover, Gd·**4** shows a very good stability, similar to that of the macrocyclic Gd·DOTA complex.

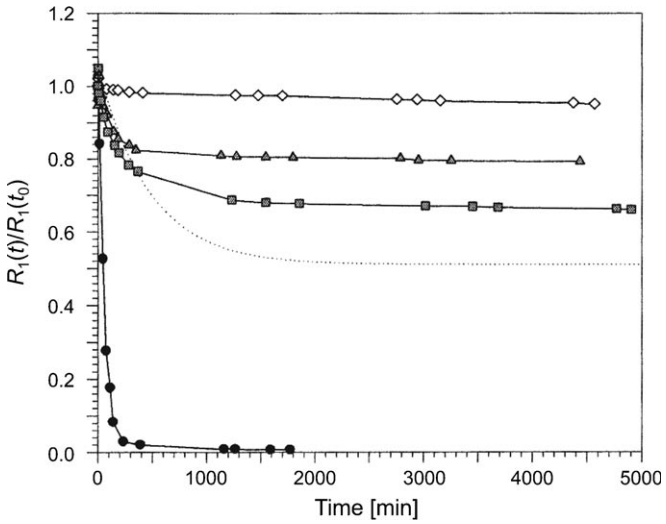

Fig. 2. *Evolution of the transmetallation process by Zn ions* vs. *time.* ···: Gd·DTPA; ○: Gd·**1**; □: Gd·**2**; △: Gd·**3**; ◇: Gd·**4**.

*Interaction with HSA. Proton Relaxation Method. Complex Gd·***1**. In the presence of HSA, it was not necessary to add EtOH in order to obtain a clear solution. As compared to the solution without HSA, the proton relaxation rates are greater over the whole magnetic field range and maximum at *ca.* 20–30 MHz (*Fig. 3*,*a*). At 20 MHz, the value of R_1^p is increased by 20% (14.5 s^{-1} in H_2O and 17.4 s^{-1} in HSA solution). This slight increase indicates either an absent or a weak affinity for the protein, or the presence of a moderate interaction with the protein leading to macromolecular species of similar rotational correlation times of bound and unbound Gd complex. However, the increase of solubility in the presence of HSA supports the presence of an interaction with HSA.

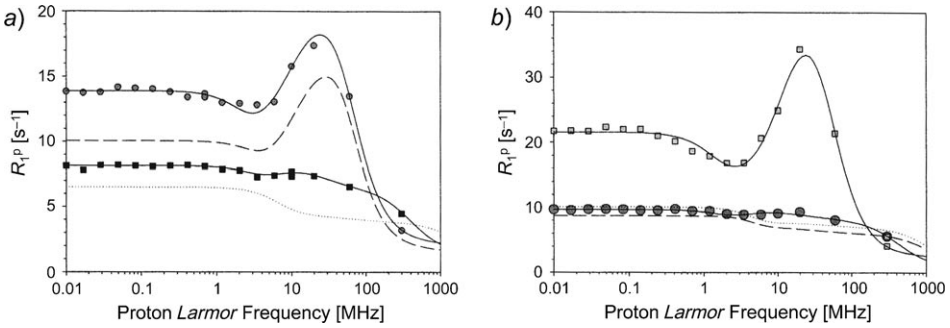

Fig. 3. *NMRD Profiles of the different complexes at a concentration of 1* mM *in the presence and absence of 4% HSA at 310 K. a*) Gd·**1** in 4% HSA (○) and in H_2O (– – –); Gd·**2** in 4% HSA (□) and in H_2O (···). *b*) Gd·**3** in 4% HSA (○) and in H_2O (– – –); Gd·**4** in 4% HSA (□) and in H_2O (···).

*Complex Gd·***2**. The R_1^p value in HSA solution shows at all fields a small increase with a slight hump at high fields reaching a R_1^p of 7.40 s^{-1} mM^{-1} at 20 MHz (*Fig. 3*,*a*).

This can be due to the increase of viscosity resulting from the presence of HSA and/or to a weak interaction between Gd·**2** and HSA.

*Complex Gd·**3***. In the presence of HSA, R_1^p increases to 9.4 s^{-1} mM^{-1} at 20 MHz (*Fig. 3,b*). As explained above for Gd·**2**, this weak change does not indicate a strong binding to HSA.

*Complex Gd·**4***. *Fig. 3,b*, shows a clear hump at high fields with an R_1^p value of 34.6 s^{-1} at 20 MHz, close to the value obtained in the literature for MS-325. This complex thus shows a marked affinity for HSA. The binding of Gd·**4** to HSA was, therefore, investigated more deeply *in vitro* by measuring the R_1^p evolution of 4% HSA solutions containing increasing amounts of Gd·**4**. This quantification of the interaction was performed at 20 MHz, the frequency range of the NMRD profile where the effect of the interaction is maximal. In pure H_2O, the relaxation rates of Gd·**4** increased linearly with the concentration, and a relaxivity (r_1) of 7.2 s^{-1} mM^{-1} was determined. When HSA is present, the increase of R_1^p is much higher and not linear, in agreement with a strong binding. The fitting of the titration data using *Eqn. 1* gave a *K* value of *ca.* 9410 ± 2560 M^{-1} with 2.0 ± 0.2 equiv. and independent binding sites and an r_1^c value of 43.0 ± 2.4 s^{-1} mM^{-1} (*Fig. 4*).

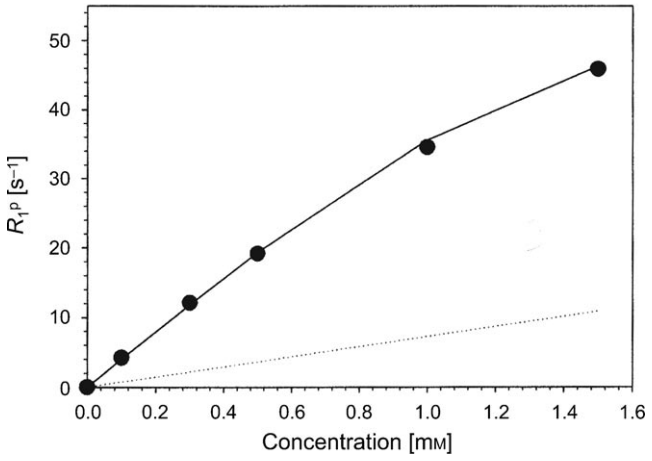

Fig. 4. *Evolution of the paramagnetic relaxation rate of H_2O H-atoms in the presence of various concentrations of Gd·[4-(carboxyundecylisothiourea-Bz)DTPA]* (Gd·**4**) *without* (···) *and with 4% of HSA* (310 K, 20 MHz). The fitting was performed using *Eqn. 1* and with the lower limit of r_1^c as largest values of the apparent relaxivity (42 s^{-1} mM^{-1}).

Electrospray Mass Spectrometry (ESI-MS). The two more stable complexes Gd·**3** and Gd·**4** were investigated by ESI-MS. *Fig. 5* shows that there is no clear additional peak after addition of a fourfold excess of Gd·**3** to 5 μM HSA as compared to HSA alone, although some broadening of the peak is observed. These data reflect an absence of or a weak interaction between the Gd complex and HSA, and agree with the relaxometric results.

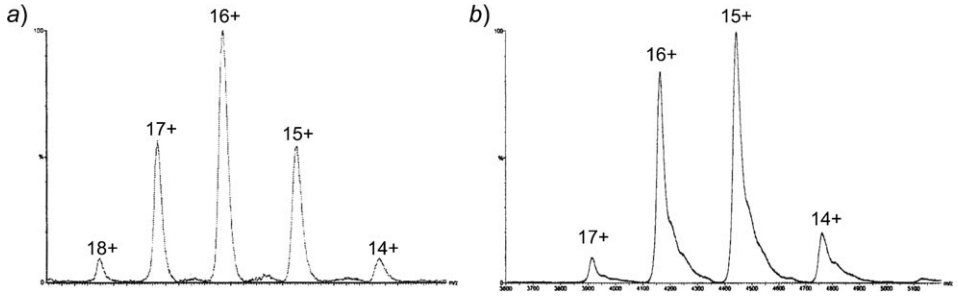

Fig. 5. *ESI Mass spectrum of* a) *HSA* (5 μM) *and* b) *HSA* (5 μM) *with Gd·[4-(dodecylisothiourea-Bz)DTPA]* (Gd·**3**) *at a concentration of 20 μM*

On the contrary, under the same conditions, when Gd·**4** is added to HSA solution several additional peaks are clearly detected (*Fig. 6,c*), indicating the presence of a strong binding of the Gd complex to HSA and the presence of several stoichiometries. When the concentrations of Gd·**4** and HSA are equal (5 μM; *Fig. 6,a*), three signals are seen in each massive: the first signal on the left hand side corresponds to the protein alone, the larger signal corresponds to a complex between the protein and one molecule of contrast agent, and the weaker signal on the right hand side results from a complex with a stoichiometry 1:2. When the concentration of contrast agent is increased to 10 μM (*Fig. 6,b*), the intensity of the signal corresponding to the protein alone decreased, and a new stoichiometry appeared. With a greater excess of contrast agent, additional stoichiometries appeared (*Fig. 6,c*). These data confirm the significant interaction of Gd·**4** with HSA and the presence of several binding sites.

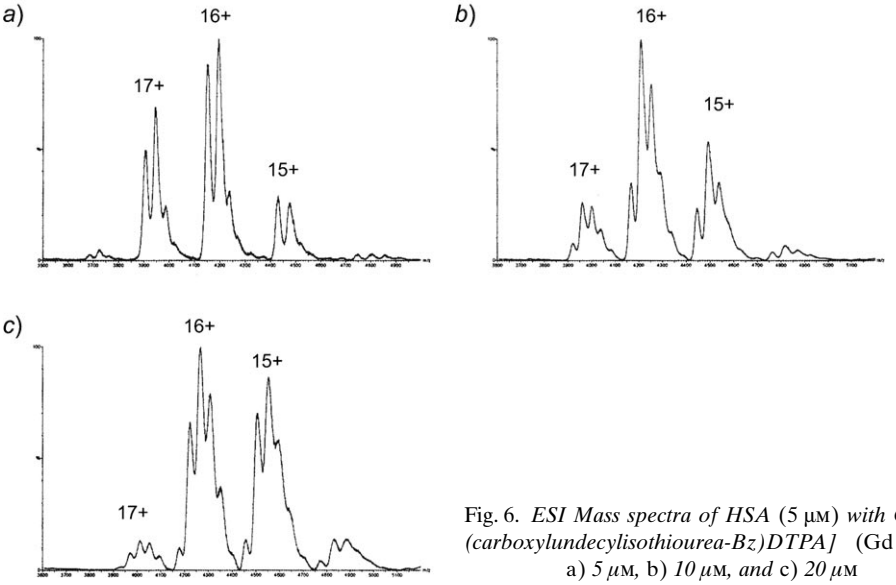

Fig. 6. *ESI Mass spectra of HSA* (5 μM) *with Gd·[4-(carboxylundecylisothiourea-Bz)DTPA]* (Gd·**4**) *at* a) *5 μM,* b) *10 μM, and* c) *20 μM*

Conclusions. – These data confirm the better stability of Gd·(4-substituted DTPA) derivatives as compared to bis[amide] ones. They also demonstrate *i*) that the presence of a negative charge on the hydrophobic alkyl chain of the Gd·(4-substituted DTPA) derivative is essential for a marked interaction with HSA, and *ii*) that bis[amide] derivatives do not bind efficiently to HSA even when the alkyl chains terminates by a negatively charged group. In conclusion and as already reported, the grafting of substituents on the 4-position of Gd·DTPA is beneficial regarding both the stability versus zinc transmetallation and the potential interaction with albumin.

The authors thank Mrs. *Patricia de Francisco* for her help in preparing the manuscript. This work was supported by the *FNRS* and the *ARC Program* 05/10-335 of the French Community of Belgium. The support and sponsorship concerted by *COST Action D38* '*Metal-Based Systems for Molecular Imaging Applications*' and the *EMIL* program are kindly acknowledged.

Experimental Part

Chemicals. 1-(4-Isothiocyanatobenzyl)diethylenetriaminepentaacetic acid was purchased from *Macrocyclics* (Dallas, USA). 12-Aminododecanoic acid and dodecanamine, and non-defatted HSA (A-1653) were purchased from *Sigma-Aldrich* (B-Bornem). All reagents were commercially available (*Aldrich* or *Fluka*, B-Bornem) and were used without further purification.

Instruments. ^{1}H- and ^{13}C-NMR Spectra: *Bruker AMX 300* spectrometer; recorded in $CDCl_3$ rel. to Me_4Si; δ in ppm, J in Hz. ESI-MS: *Q-TOF 2* or *Q-TOF Ultima* (*Micromass*, Manchester, UK); samples were solubilized in MeOH. Proton Relaxometry: NMRD Profiles were obtained at 310 K on a fast field cycling relaxometer (*Stelar*, I-Mede). The range of magnetic fields covered extends from 0.24 mT to 0.24 T, which corresponds to frequencies varying from 0.01 to 10 MHz. Additional longitudinal relaxation rates were measured on *Bruker Minispecs mq20* and *mq60*, and *Bruker AMX-300* spectrometer at 20 MHz (0.47 T), 60 MHz (1.41 T), and 300 MHz (7.05 T), resp.

The data were analyzed using the classical description which takes into account two contributions: the inner-sphere model described by *Solomon* [8] and *Bloembergen* [9], which refers to short-distance interactions, and the outer-sphere contribution described by *Freed* [10], which accounts for the larger-distance interactions. Various parameters related to the structure and the dynamics of the complex are used in these models. Some of them are quite similar for all low-molecular-weight complexes, like the distance of closest approach ($d = 0.36$ nm), the distance between the H-atoms of the coordinated H_2O molecules and the Gd-atom ($r = 0.30–0.31$ nm), and the relative diffusion constant which is close to the value of pure H_2O ($D = 3.0 \times 10^{-9}$ m^2 s^{-1} at 310 K) [11]. The structure of the complex determines other parameters, *i.e.*, q, the number of coordinated H_2O molecules; τ_M, the residence time of these H_2O molecules; τ_R, the rotational correlation time of the complex; τ_{SO}, the electronic relaxation time at very low fields; and τ_V, the correlation time describing the modulation of the zero-field splitting (ZFS).

The evolution of the transmetallation process was followed by proton relaxometry on a *Minispec* 20 MHz as described in [15][16].

Studies of Noncovalent Interactions. Proton Relaxivity Method. The proton relaxation rates (R_{1obs}) were measured at a fixed field strength (0.47 T) and temp. (310 K) using a *Minispec* (*Bruker*, D-Karlsruhe). The HSA concentration was set to 0.6 mM (4%), and the concentration of contrast agents ranged from 0 to 2 mM. The proton data obtained in HSA solution were fitted using *Eqn. 1*.

$$R_{1obs}^{P} = 1000\left[r_1^f L_0 + \left(r_1^c - r_1^f\right)\left\{\frac{NP_0 + L_0 + K^{-1} - \sqrt{(NP_0 + L_0 + K^{-1})^2 - 4L_0P_0}}{2}\right\}\right] \quad (1)$$

where R_{1obs}^{P} is defined as the observed relaxation rate minus the proton relaxation rate of the solution without contrast agent, K is the association constant, P_0 is the protein concentration, L_0 is the concentration of the paramagnetic complex studied, N is the number of independent and identical

interaction sites, and r_1^c and r_1^f [s^{-1} mM^{-1}] are the relaxivities of the complex HSA–contrast agent and the free contrast agent, resp.

ESI-MS Method. The nanospray source was operated in the pos.-ion mode at a cap. voltage of 1.4 kV. The samples, dissolved in $AcONH_4$ (50 mM), were injected through needles at a flow rate of a few nl/min. For this procedure, HSA was desalted by five dilution-concentration steps using *Microcon YM-10* from *Millipore* (B-Brussels). The concentration of albumin samples, measured by spectrophotometry (UV, λ 280 nm; *8452A* diode array spectrophotometer *Hewlett-Packard*, B-Brussels), injected into the mass spectrometer was 5 μM. Each spectrum is the sum of *ca.* 400 scans.

Synthesis of Gd Complexes. Ligands. The DTPA bisamides were synthesized as described in the literature [6][17], and their structures were confirmed by proton and carbon-13 NMR spectroscopy and mass spectrometry.

DTPA-BdodecylAmide (*=6-(Carboxymethyl)-3,9-bis[2-(dodecylamino)-2-oxoethyl]-3,6,9-triazaundecanedioic Acid*; **1**). ^{1}H-NMR: 8–7.6 (*m*, 3 OH, 2 NH); 3.7–2.9 (*m*, 11 CH_2); 1.5 (*m*, 2 CH_2); 1.4–1.1 (*m*, 18 CH_2); 0.9 (*m*, 3 CH_2). ^{13}C-NMR: 178.2; 177.1; 170.1; 59.9; 58.7; 57.8; 56.4; 52.6; 38.9; 31.9; 29.7; 29.6; 29.5; 29.3; 28.9; 26.3; 25.7; 25.6; 22.7; 14.1. ESI-MS: 728 ($[M+H]^+$).

DTPA-BcarboxylundecylAmide (*=16,19,22-Tris(carboxymethyl)-14,24-dioxo-13,16,19,22,25-pentaazaheptatriacontanedioic Acid*; **2**). ^{1}H-NMR: 8.1–7.7 (*m*, 5 OH, 2 NH); 3.5–3 (*m*, 11 CH_2); 2.4–2.2 (*m*, 2 CH_2); 1.5 (*m*, 2 CH_2); 1.4–1.1 (*m*, 18 CH_2). ^{13}C-NMR: 181.7; 179.8; 176.2; 170.5; 59.9; 58.8; 57.9; 52.3; 49.9; 45.8; 38.9; 34.1; 30.7; 30.1; 29.6; 29.4; 28.8; 26.3; 25.7; 23.6. ESI-MS: 832 ($[M+2Na]^+$).

Ligands **3** and **4** were synthesized by adding an aq. soln. of dodeanamide and aminolauric acid, resp., to a soln. of 1-(4-isothiocyanatobenzyl)diethylenetriaminepentaacetic acid (1.5 equiv.). The pH of the soln. was set between 9 and 10, and the soln. was stirred for 48 h at r.t. After reaction, the product was dialyzed on a *spectra/Por® Biotech Cellulose Ester* (CE) membrane with a cut-off of 500 (*VWR*, B-Leuven) and purified by column chromatography (CC) on silica gel *60 RP-18* (40–63 μm; *Merck*, D-Darmstadt) with MeOH/H_2O 40:60 (*v/v*).

4-(Dodecylisothiourea-Bz)DTPA (= N-*(2-[Bis(carboxymethyl)amino]-3-{4-[(dodecylcarbamothioyl)amino]phenyl}propyl)*-N-*{2-[bis(carboxymethyl)amino]ethyl}glycine*; **3**). ^{1}H-NMR: 7.2–6.8 (*AA′BB′*, 4 arom. H); 5 (*quint.*, CH); 4 (*s*, 2 CH_2); 3.7 (*s*, CH_2); 3.5–3.4 (*m*, 2 CH_2); 3.3 (*s*, 2 CH_2); 2.9–2.5 (*m*, 3 CH_2); 1.7–1.5 (*m*, 2 CH_2); 1.4–1.3 (*m*, 8 CH_2); 0.9 (*t*, Me). ^{13}C-NMR: 181.9; 177.8; 175.5; 170.6; 138.5; 133.1; 130.6; 118.7; 61.1; 60.6; 58.9; 57.1; 56.7; 52.9; 49.6; 44.5; 40.8; 33.1; 31.9; 30.1; 29.7; 29.5; 29.4; 29.1; 28.8; 22.7; 14.1. ESI-MS: 727 ($[M+H]^+$).

4-(Carboxylundecylisothiourea-Bz)DTPA (*=12-{[(4-{2-[Bis(carboxymethyl)amino]-3-[{2-[bis(carboxymethyl)amino]ethyl}(carboxymethyl)amino]propyl}phenyl)carbamothioyl]amino}dodecanoic Acid*; **4**). ^{1}H-NMR: 7.1–6.7 (*AA′BB′*, 4 arom. H); 5 (*quint.*, CH); 4 (*s*, 2 CH_2); 3.7 (*s*, CH_2); 3.5–3.4 (*m*, 2 CH_2); 3.3 (*s*, 2 CH_2); 2.9–2.5 (*m*, 3 CH_2); 2.3 (*t*, CH_2); 1.7–1.5 (*m*, 4 CH_2); 1.4–1.3 (*m*, 7 CH_2). ^{13}C-NMR: 182.7; 182.0; 177.5; 175.5; 170.6; 138.5; 133.4; 130.6; 118.7; 61.1; 60.5; 58.4; 57.1; 56.7; 53.4; 49.6; 44.5; 40.8; 34.0; 31.9; 30.1; 30.0; 29.6; 29.4; 29.1; 28.9; 23.6. ESI-MS: 757 ($[M+H]^+$).

Complexes. Equimolar amounts of ligand (1 mmol) [6] and $GdCl_3 \cdot 6\,H_2O$ were mixed. The pH was adjusted to 5 with pyridine, and the soln. was stirred overnight. The soln. was filtered, and the solvent was evaporated under vacuum. Xylenol or arsenazo tests confirmed the absence of free Gd [18]. The product was treated with 50 ml of dist. H_2O and then lyophilized, and its structure was confirmed by MS. The complex was desalted by dialysis on membranes with a molecular weight cutoff (MWCO) value of 500.

Gd·DTPA-BdodecylAmide (Gd·**1**). HR-ESI-MS: 883.4548 ($[M+H]^+$, $C_{38}H_{71}GdN_5O_8^+$; calc. 883.4544).

Gd·DTPA-BcarboxylundecylAmide (Gd·**2**). HR-ESI-MS: 941.3869 ($[M+H]^+$, $C_{38}H_{65}GdN_5O_{12}^+$; calc. 941.3871).

Gd·(4-(Dodecylisothiourea-Bz)DTPA) (Gd·**3**). HR-ESI-MS: 925.2379 ($[M+H]^+$, $C_{34}H_{51}GdN_5Na_2O_{10}S^+$; calc. 925.2393).

Gd·(4-(Carboxylundecylisothiourea-Bz)DTPA) (Gd·**4**). HR-ESI-MS: 977.1959 ($[M+H]^+$, $C_{34}H_{47}GdN_5Na_3O_{12}S^+$; calc. 977.1954).

REFERENCES

[1] R. B. Lauffer, D. J. Parmelee, H. S. Ouellet, R. P. Dolan, H. Sajiki, D. M. Scott, P. J. Bernard, E. M. Buchanan, K. Y. Ong, Z. Tyeklár, K. S. Midelfort, T. J. McMurry, R. C. Walovitch, *Acad. Radiol.* **1996**, *3*, S356.

[2] R. N. Muller, B. Radüchel, S. Laurent, J. Platzek, C. Piérart, P. Mareski, L. Vander Elst, *Eur. J. Inorg. Chem.* **1999**, 1949.

[3] P. Caravan, N. J. Cloutier, M. T. Greenfield, S. A. McDermid, S. U. Dunham, J. W. M. Bulte, J. C. Amedio Jr., R. J. Looby, R. M. Supkowski, W. De W. Horrocks, T. J. McMurry, R. B. Lauffer, *J. Am. Chem. Soc.* **2002**, *124*, 3152.

[4] M. Goyen, M. Edelman, P. Perreault, E. O'Riordan, H. Bertoni, J. Taylor, D. Siragusa, M. Sharafuddin, E. R. Mohler III, R. Breger, E. K. Yucel, K. Shamsi, R. M. Weisskoff, *Radiology* **2005**, *236*, 825.

[5] G. Sudlow, D. J. Birkett, D. N. Wade, *Mol. Pharmacol.* **1976**, *12*, 1052.

[6] K. Kimpe, T. N. Parac-Vogt, S. Laurent, C. Piérart, L. Vander Elst, R. N. Muller, K. Binnemans, *Eur. J. Inorg. Chem.* **2003**, 3021.

[7] C. Henoumont, V. Henrotte, S. Laurent, L. Vander Elst, R. N. Muller, *J. Inorg. Biochem.* **2008**, *102*, 721.

[8] I. Solomon, *Phys. Rev.* **1955**, *99*, 559.

[9] N. Bloembergen, *J. Chem. Phys.* **1957**, *27*, 572.

[10] J. H. Freed, *J. Chem. Phys.* **1978**, *68*, 4034.

[11] L. Vander Elst, A. Sessoye, S. Laurent, R. N. Muller, *Helv. Chim. Acta* **2005**, *88*, 574.

[12] L. Vander Elst, F. Maton, S. Laurent, F. Seghi, F. Chapelle, R. N. Muller, *Magn. Reson. Med.* **1997**, *38*, 604.

[13] S. Laurent, L. Vander Elst, S. Houzé, N. Guérit, R. N. Muller, *Helv. Chim. Acta* **2000**, *83*, 394.

[14] S. Laurent, F. Botteman, L. Vander Elst, R. N. Muller, *Eur. J. Inorg. Chem.* **2004**, 463.

[15] S. Laurent, L. Vander Elst, F. Copoix, R. N. Muller, *Invest. Radiol.* **2001**, *36*, 115.

[16] S. Laurent, L. Vander Elst, R. N. Muller, *Contrast Media Mol. Imaging* **2006**, *1*, 128.

[17] W. P. Cacheris, R. C. Grabiak, A. C. Lee, T. J. Richard, T. H. Goodin, R. J. Kaufman, 'Emulsions of Lipophilic Paramagnetic Complexes as MRI Contrast Media', in 'Proceedings of the 4th Special Topic Seminar of the European Magnetic Resonance Forum', Eds. P. A. Rinck, R. N. Muller, 1994, pp. 37–51.

[18] A. Barge, G. Cravotto, E. Gianolio, F. Fedeli, *Contrast Media Mol. Imaging* **2006**, *1*, 184.

Received July 10, 2010